Magazine of Civil Engineering

ISSN 2712-8172

journal homepage: http://engstroy.spbstu.ru/

Research article

UDC 539.3

DOI: 10.34910/MCE.138.8

Parameter identification of the concrete damaged plasticity model

I.R. Murtazin[1] ✉ , ***R.V. Fedorenko***[1] , ***A.V. Lukin***[1] , ***V.S. Modestov***[1] , ***A.S. Malinkin***[2], ***M.A. Fedotov***[2], ***S.N. Panarin***[2]

[1] *Peter the Great St. Petersburg Polytechnic University, St. Petersburg, Russian Federation*

[2] *TEKHNOARM+, St. Petersburg, Russian Federation*

✉ *murtazin_ir@spbstu.ru*

Keywords: parameter identification, stress-strain curve, cyclic loading, concrete damage, analytical approximation, ABAQUS

Abstract. The article is devoted to the development of methods for identification and validation of the parameters of the "Concrete Damage Plasticity" material model based on experimental studies. During the experiments, prismatic samples were tested for sign-constant cyclic load after preliminary heat treatment at various temperatures. According to the test results, the temperature dependences of the mechanical properties were established: the conditional proportionality limit, the ultimate strength, Young's modulus, and the scalar damage variable. Piecewise analytical envelopes were used to plot the stress-strain curves, which describe linear, inelastic, and descending parts. Accumulated concrete scalar damage variable during compression is determined based on the elastic modulus degradation analysis at each loading cycle. Parameters of analytical approximations are determined directly through experimental data or using numerical identification method based on an iterative process of searching for the minimum functional. The structure of the minimized functional contains auxiliary subfunctions due to well-known statistical indicators: the standard deviation of the compared values, the linear correlation coefficient, and the area under the compared dependencies. The search for the minimum of the desired value is carried out using the gradient descent method according to the criterion of the minimum contribution of the sum of three subfunctions. At the last step of the study, the obtained model is validated based on the calculation for uniaxial and cyclic loading of a single-element prismatic sample in the ABAQUS FEA. The developed calculation method makes it possible to complete the loading cycle at any axial force value, including zero, as well as to continue the next loading cycle from the current stress state. The considered method for validating the inelastic deformation model for concrete is characterized by its consistency and versatility. The results demonstrate sufficient accuracy in approximating uniaxial and cyclic stress-strain curves, and the proposed approximation relationships are free from ambiguity when converting the inelastic part of strain to plastic one.

Funding: World-class Research Center program: Advanced Digital Technologies, No. 075-15-2022-311 dated 20.04.2022

Citation: Murtazin, I.R., Fedorenko, R.V., Lukin, A.V., Modestov, V.S., Malinkin, A.S., Fedotov, M.A., Panarin, S.N. Parameter identification of the concrete damaged plasticity model. Magazine of Civil Engineering. 2025. 18(6). Article no. 13808. DOI: 10.34910/MCE.138.8

1. Introduction

Today, mechanical design methods are characterized by increased requirements for safety and wear resistance, especially during operation in high-temperature conditions. Along with this, the issue of correctly

assessing the viability of critical elements of structures is becoming acute. It is impossible to imagine solving such problems without carrying out full-scale tests and numerical modeling procedures using modern computational environments.

One of the main structural materials is concrete. A distinctive feature of concrete is its fundamentally different behavior during compression and tension, as well as the phenomenon of cracks and damage formation and propagation [1–3]. Tests for cyclic sign-constant loading without transition to the tensile region make it possible to determine the main mechanical characteristics of the material – the initial Young modulus, the conditional proportionality limit, the compressive strength of concrete, as well as to identify the material stiffness degradation by determining the dependence of the scalar variable of accumulated damage on the magnitude of inelastic deformations [4–7]. It is often important to understand how the key characteristics of a structure change under thermal conditions. In this case, it is about a family of experiments for different temperature values [8]. The numerical modeling of inelastic deformation processes is based on mathematical models. One of the most wide-spread models for concrete is the "Concrete Damaged Plasticity" (CDP) model [9–13], implemented in the ABAQUS FEA [14]. The model is widely used and finds its application in many tasks related to the deformation and fracture of concrete and concrete-like (with a granular structure) materials [15–21].

This model considers inelastic behavior in both compression and tension and takes into account not only material damage [22–24] but also partial recovery of properties during reverse-sign loading [25]. The CDP model is purposed for calculating structures under the influence of monotonous, cyclic, and dynamic loads.

Analytical approximations are often used to describe compression diagrams and scalar damage variables [25–27]. A distinctive feature of such approaches is the unambiguous relationship between plastic and inelastic strain. In contrast to the case of an arbitrarily defined envelope of the diagram, such a relationship eliminates the disadvantages associated with the decrease, including to negative values, of plastic strain when they are recalculated from inelastic ones. In addition to the basic constants of the material, the parameters included in the approximation dependences are also subject to identification.

As already mentioned, some model parameters are explicitly defined based on existing dependencies. However, a more sophisticated approach is required to determine the proportion of plastic strain contained in the inelastic part. In this case, the algorithm proposed in [28] was used as the basis for the identification procedure. In the current work, a modified criterion is used, presented as the sum of the simplest ones.

Using the interpolation method, the obtained parameters make it possible to form universal analytical dependencies for arbitrary temperature values. The corresponding curves are supposed to be used for the verification task in the ABAQUS FEA. The kinematic loading of a single-element prismatic sample for uniaxial and cyclic action is assumed. The criterion for the model's operability in this case will be the coincidence of the sample response in terms of stress and strain, as well as the nature of the Young modulus (stiffness) degradation with the initially set properties.

2. Methods

2.1. Processing of Experimental Data

During the experiments, prismatic concrete samples of 70×70×280 mm were tested for cyclic sign-constant compression until failure under normal conditions (20 °C), as well as after heat treatment at temperatures of 100, 400, and 600 °C in a cooled state. The tests were carried out on samples of heat-resistant concrete from a self-sealing mixture.

The amount of deformation of the samples during their loading/unloading was measured using digital electronic indicators mounted on each side of the prismatic sample according to a scheme similar to that used to determine the Young modulus of concrete. The load value was determined by a compression dynamometer. The readings were recorded at a sampling rate of 140 ms using a hardware and software package developed separately for this task.

Figs. 1 and 2 show the condition of the samples after the first and last loading cycle for temperatures of 20 and 600 °C.

Figure 1. The state of the sample after the first (left) and last (right) loading cycle at a temperature of 20 °C.

Figure 2. The state of the sample after the first (left) and last (right) loading cycle at a temperature of 600 °C.

Primary processing of cyclic loading diagrams involves finding the ultimate strength, the conditional proportionality limit, and analyzing the Young modulus (stiffness) degradation. The conditional proportionality limit here is a value equal to 0.4 of the ultimate strength.

Fig. 3 shows the cyclic loading diagrams for the given temperatures, as well as the initial modulus of normal elasticity and its degradation, the conditional limit of proportionality and the ultimate strength.

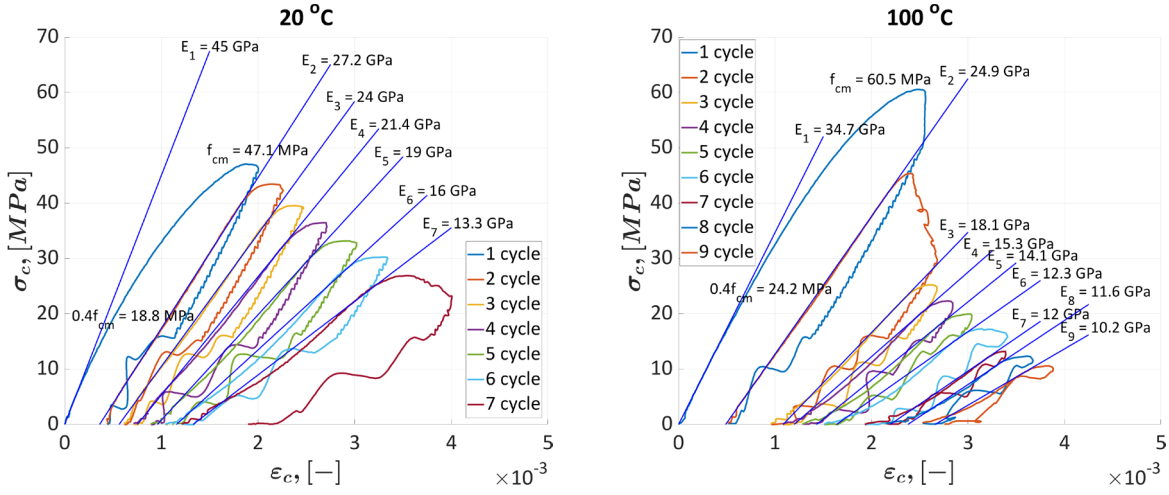

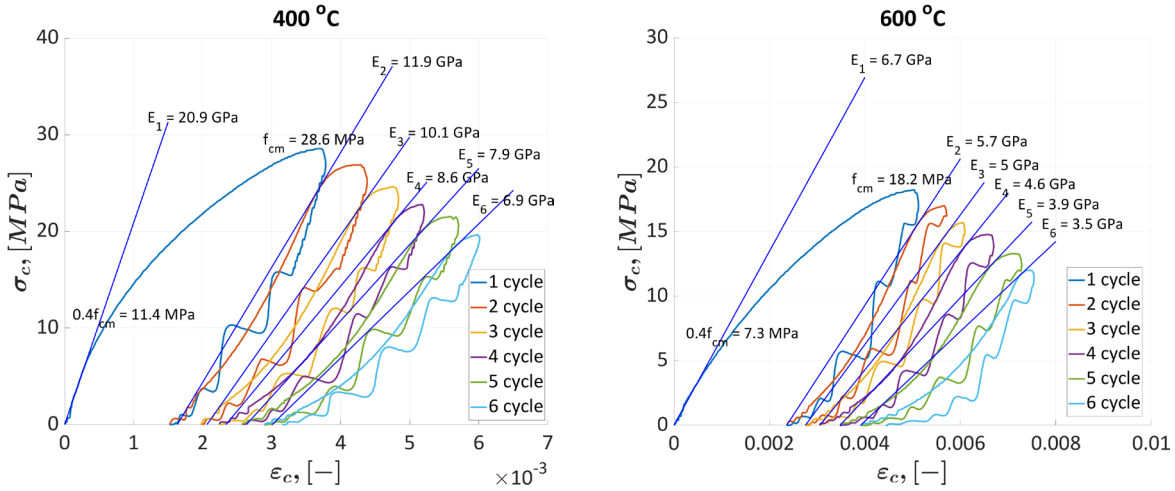

Figure 3. Cyclic loading diagrams for the given temperatures with designations of the ultimate strength f_{cm}, the conditional proportionality limit 0.4 f_{cm}, and the evolution of Young modulus.

Here σ_c is the compression normal stress, ε_c is the total axial strain, E_i is the Young modulus at the i-th cycle.

It is worth noting that the plotting of slope lines at each cycle characterizing the linear-elastic part can be carried out both along the unloading and loading path [26]. In this case, a variant of the slope of the line following from the end of unloading (the beginning of the next loading cycle) to the point where the dependence, having a negative second derivative, begins to acquire a non-linear character.

Based on the diagrams shown, it is easy to form the dependences of the scalar damage variable on inelastic strain. Inelastic strain can be recalculated through total ones according to the relation (1) [5, 6, 14, 26]:

$$\varepsilon_c^{in} = \varepsilon_c - \frac{\sigma_c}{E_c}, \tag{1}$$

where $E_c \equiv E_1$ is the initial Young modulus.

At the same time, the relationship between the actual Young modulus at the i-th cycle and the initial one is determined by dependence (2) [5, 6, 16]:

$$E_i = \left(1 - d_c\right) E_c, \tag{2}$$

where $d_c = d_c\left(\varepsilon_c^{in}\right)$ is the scalar damage (stiffness degradation) variable.

In addition to inelastic strain, the plastic component is separately identified. It is obviously less than inelastic one when taking into account damage, but in the absence of such, these values are the same. In this case, plastic strain cannot be negative and must increase with increasing load. Plastic component of strain is related to total and inelastic according to expression (3) [27]:

$$\varepsilon_c^{pl} = \varepsilon_c - \frac{\sigma_c}{\left(1 - d_c\right) E_c} = \varepsilon_c^{in} - \frac{1}{\left(1 - d_c\right)} \frac{\sigma_c}{E_c}. \tag{3}$$

Being a function of inelastic strain, the parameter d_c is calculated at each loading cycle using expression (2) for a given value of ε_c^{in}. By performing this procedure for each diagram, a family of dependencies is obtained for each temperature. Fig. 4 shows a family of dependencies of the scalar damage variable on inelastic strain for temperatures of 20, 100, 400, and 600 °C. It is clear that $d_c\left(0\right) = 0$.

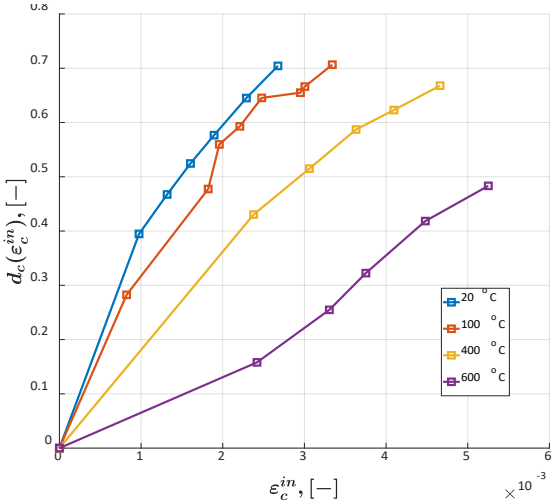

Figure 4. Family of dependencies of scalar damage variable on inelastic strain for temperatures of 20, 100, 400, and 600 °C.

The obtained characteristics fully correspond to the experiments, however, for the setting of numerical procedures, they require more detailed analysis. This is primarily due to the features of the CDP model. For the full-fledged operation of the model, at least it is necessary to specify the basic elastic characteristics, a stress-strain curve describing nonlinear (including plastic) strain, as well as information on the initial stiffness properties degradation for optional damage accounting. At the same time, the specified characteristics should not contradict the basic principles of mechanics of a deformable solid.

So, not every arbitrarily defined envelope of a cyclogram can correspond to an adequate relationship between the plastic and inelastic parts of strain, as well as to a given law of properties degradation (equation (3)). In this case, it is more reasonable to use analytical approximations, which, when implemented in constitutive equation, obviously eliminate these disadvantages.

2.2. Analytical Dependencies

Expressions (1)–(3) underlie the dependence of normal compression stress on relative axial strain, taking into account damage [25] in the form of expression (4):

$$\sigma_c = \left(1 - d_c\right) E_c \left(\varepsilon_c - \varepsilon_c^{pl}\right). \tag{4}$$

The difference between a model of a material with plasticity, a model of a material with damage, and a model of a material with damage and plasticity is best demonstrated in Fig. 5 [25].

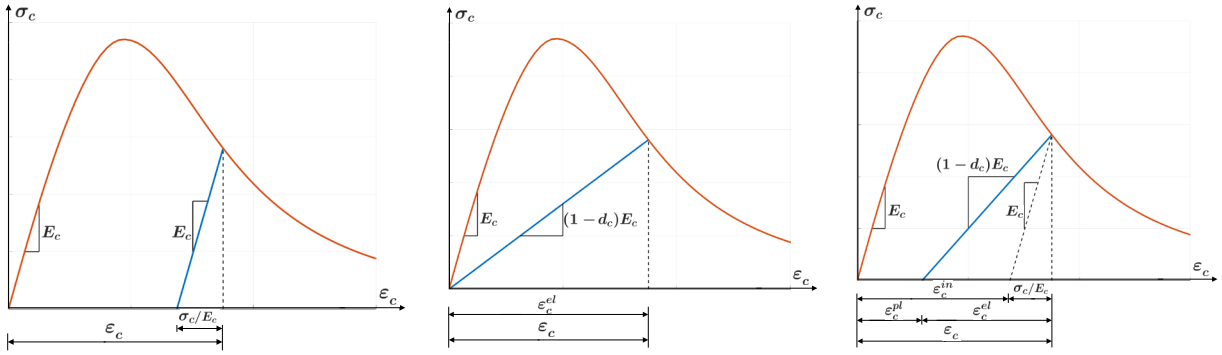

Figure 5. Comparison of model behavior: material model with plasticity (left), material model with damage (middle), and material model with damage and plasticity (right).

Here ε_c^{el} is the total elastic strain.

For the analytical description of stress-strain curves, piecewise analytical dependencies (5)–(7) are used [26]. The diagram is divided into three sections: the linear-elastic section, the ascending part up to the ultimate strength, and the descending part. A division into sections scheme can be seen in Fig. 6 [26].

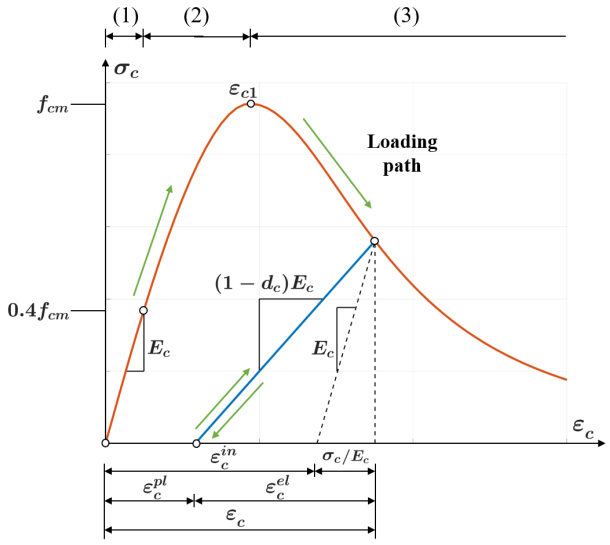

Figure 6. Piecewise analytical partition of a stress-strain curve.

Here ε_{c1} is the ultimate compression strain.

$$\sigma_{c(1)} = E_c \varepsilon_c; \tag{5}$$

$$\sigma_{c(2)} = \frac{E_{ci}\dfrac{\varepsilon_c}{f_{cm}} - \left(\dfrac{\varepsilon_c}{\varepsilon_{c1}}\right)^2}{1 + \left(E_{ci}\dfrac{\varepsilon_c}{f_{cm}} - 2\right)\dfrac{\varepsilon_c}{\varepsilon_{c1}}}; \tag{6}$$

$$\sigma_{c(3)} = \left(\frac{2 + \gamma_c f_{cm}\varepsilon_{c1}}{2 f_{cm}} - \gamma_c \varepsilon_c + \frac{\gamma_c \varepsilon_c^2}{2\varepsilon_{c1}}\right)^{-1}, \tag{7}$$

where E_{ci}, γ_c are the parameters of analytical approximations to be identified.

The relationship between the scalar damage variable and inelastic (or plastic) strain is obtained from the expression (3):

$$d_c = 1 - \frac{\sigma_c / E_c}{\left(\varepsilon_c^{in} + \varepsilon_c^{pl}\right) + \sigma_c / E_c}. \tag{8}$$

From expression (3) and Fig. 6, it can be seen that plastic strain, taking into account damage, is obviously less than inelastic one. This gives reason to believe that one can be expressed through the other using the proportionality coefficient. The proposed approach is outlined in [24–26] and shown in ratio (9):

$$\varepsilon_c^{pl} = b_c \varepsilon_c^{in}, \tag{9}$$

where $0 < b_c \le 1$ is the parameter of analytical approximations to be identified.

In this case, dependence (8) is transformed into the form:

$$d_c\left(\varepsilon_c^{in}\right) = 1 - \frac{\sigma_c / E_c}{\varepsilon_c^{in}\left(1 - b_c\right) + \sigma_c / E_c}. \tag{10}$$

Parameter identification is supposed to be carried out using the built-in procedures of the MATLAB computational environment.

2.3. Parameter Identification for Stress-strain Curves

To plot stress-strain diagrams, it is necessary to obtain cyclogram envelopes, the parts of which are described by expressions (5)–(8). The Curve Fitting Toolbox built into the MATLAB environment is well suited for this.

Fig. 7 shows the envelopes of the cyclograms for temperatures of 20, 100, 400, and 600 °C.

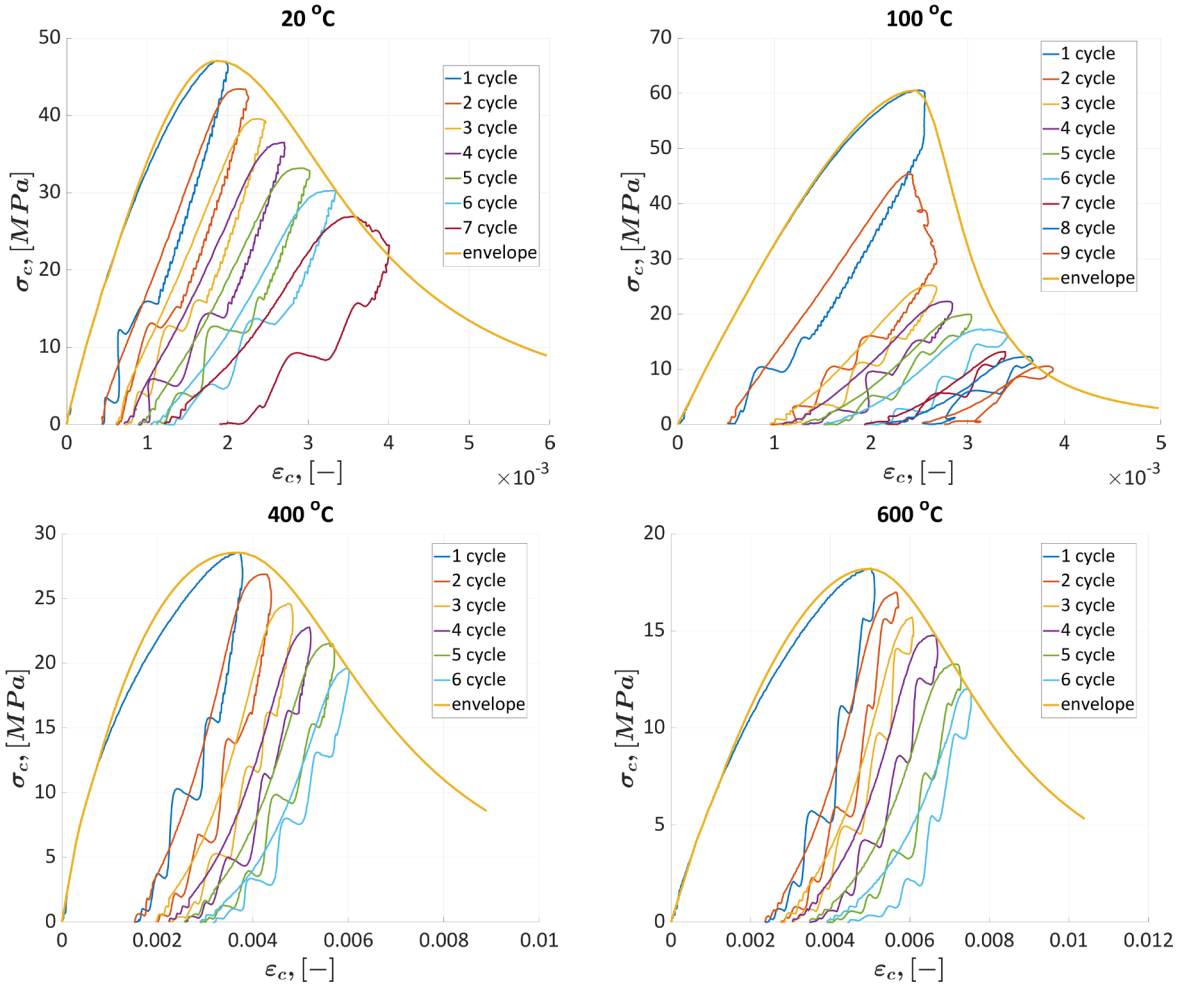

Figure 7. Cyclogram envelopes for temperatures of 20, 100, 400, and 600 °C.

The values of the selected parameters of analytical dependencies for all temperatures are presented in Table 1 of Section 2.5, as well as in Figs. 10 and 11.

2.4. Parameter Identification for Scalar Damage Variable

The identification of the b_c parameter that is present in dependence (10) is carried out based on the approach described in [28]. The *fmincon* tool implemented in the MATLAB environment, which is based on the gradient descent method, is used [29]. The algorithm block scheme is shown in Fig. 8.

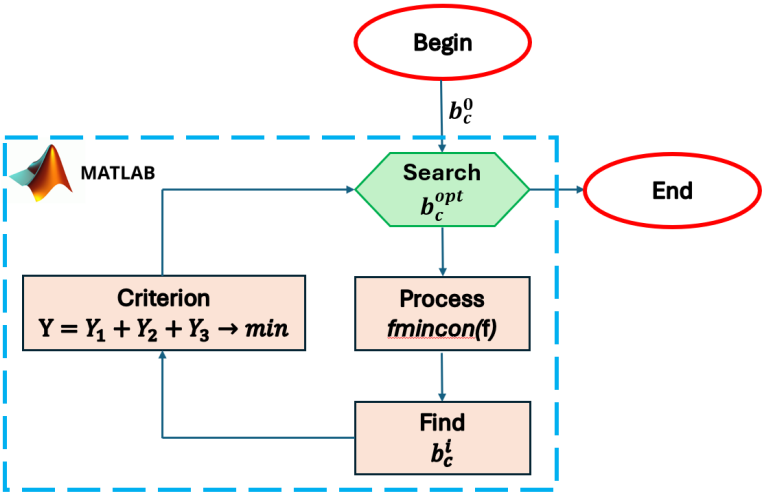

Figure 8. The b_c parameter search algorithm.

Here b_c^0 is the initial value of the parameter; b_c^i is the value of the parameter at the i-th iteration of the optimization procedure; b_c^{opt} is the optimal value of the parameter according to the criterion; Y is the minimized functional; Y_1, Y_2, Y_3 are the functionals that characterize the degree of closeness of the analytical dependence to its experimental etalon.

The functional Y_1 considers the standard deviation of two values [30]. The formulation of this functional is described by the expression (11):

$$Y_1 = \sum\left(d_c^{\exp}\left(\varepsilon_c^{in}\right) - d_c^{analyt}\left(\varepsilon_c^{in}\right)\right)^2. \tag{11}$$

The functional Y_2 considers the linear Pearson correlation coefficient between two values and its proximity to 1 [31]. The formulation of this functional is described by the expression (12):

$$Y_2 = \frac{\sum\left(d_c^{\exp}\left(\varepsilon_c^{in}\right) - \overline{d_c^{\exp}\left(\varepsilon_c^{in}\right)}\right)\sum\left(d_c^{analyt}\left(\varepsilon_c^{in}\right) - \overline{d_c^{analyt}\left(\varepsilon_c^{in}\right)}\right)}{\sum\left(d_c^{\exp}\left(\varepsilon_c^{in}\right) - \overline{d_c^{\exp}\left(\varepsilon_c^{in}\right)}\right)^2 \sum\left(d_c^{analyt}\left(\varepsilon_c^{in}\right) - \overline{d_c^{analyt}\left(\varepsilon_c^{in}\right)}\right)^2} - 1. \tag{12}$$

The functional Y_3 considers the difference in areas under dependencies. The formulation of this functional is described by the expression (13):

$$Y_3 = \int_0^{\varepsilon_{c,\max}^{in}} \left(d_c^{\exp}\left(\varepsilon_c^{in}\right) - d_c^{analyt}\left(\varepsilon_c^{in}\right)\right) d\varepsilon_c^{in}. \tag{13}$$

Fig. 9 shows a comparison of the analytical and experimental dependencies of scalar damage variables on the value of inelastic strain for temperatures of 20, 100, 400, and 600 °C. It is assumed that these dependencies will be extended to the final values of inelastic strain on corresponding stress-strain curves.

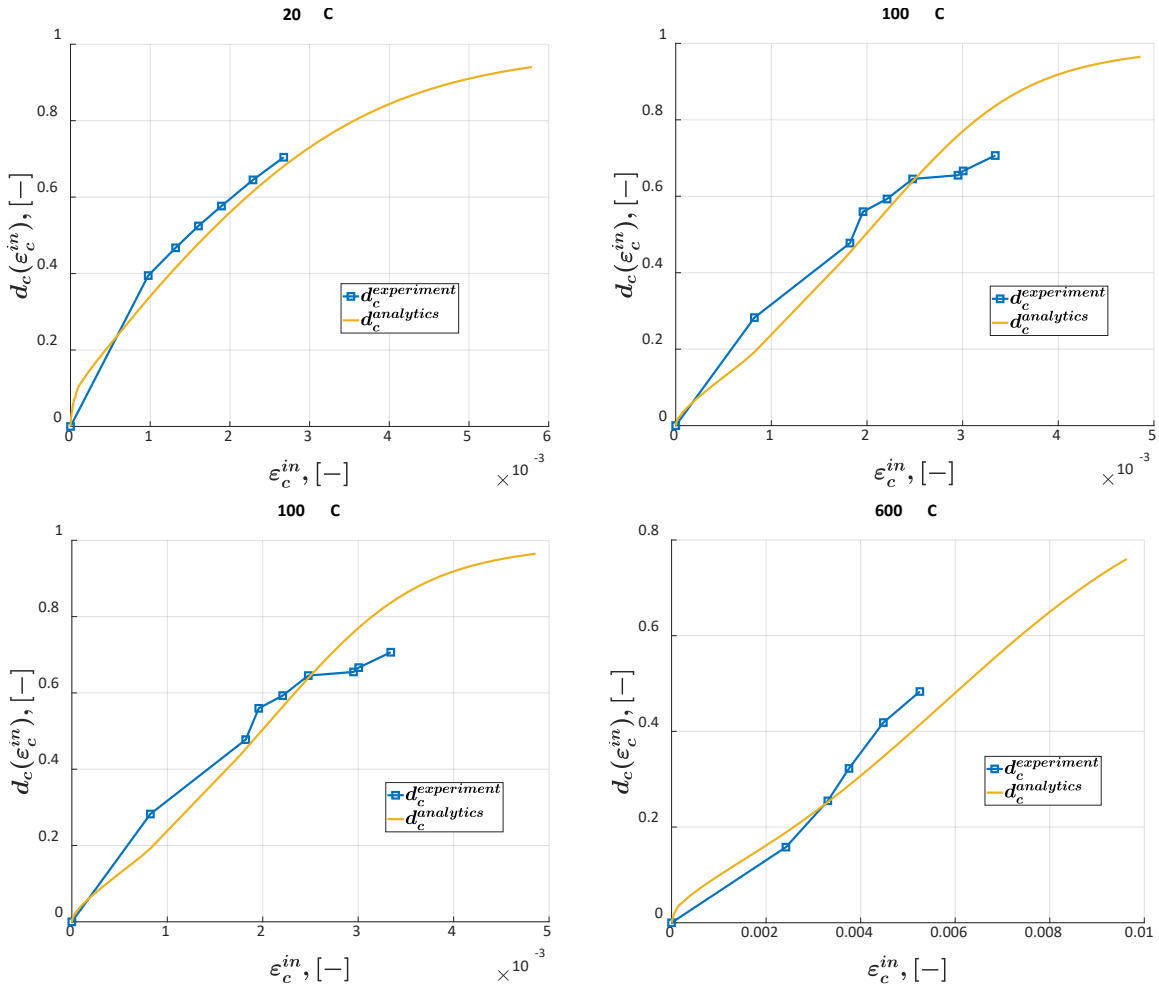

Figure 9. Comparison of analytical and experimental dependencies of scalar damage variable on the value of inelastic strain for temperatures of 20, 100, 400, and 600 °C.

The values of the b_c parameter for all temperatures are presented in Table 1 of Section 2.5, as well as in Figs. 10 and 11.

2.5. Temperature Dependencies

The obtained stress-strain and scalar damage variable curves were used in the verification of the CDP mathematical model based on the problem of uniaxial monotonic and cyclic loading of a prismatic concrete sample in the ABAQUS FEA. In problems with intense high-gradient temperature loading, due to a large gap in the temperature grid, interpolation errors can occur when determining the physical and mechanical characteristics of the material. In this regard, it is proposed to plot the obtained analytical dependencies for an extended family of temperatures. Figs. 10 and 11 show the dependence of the basic constants of the material on temperature. Using the linear interpolation method, the temperature grid is expanded from 20, 100, 400, and 600 °C to 20, 100, 150, 200, 300, 400, 500, and 600 °C.

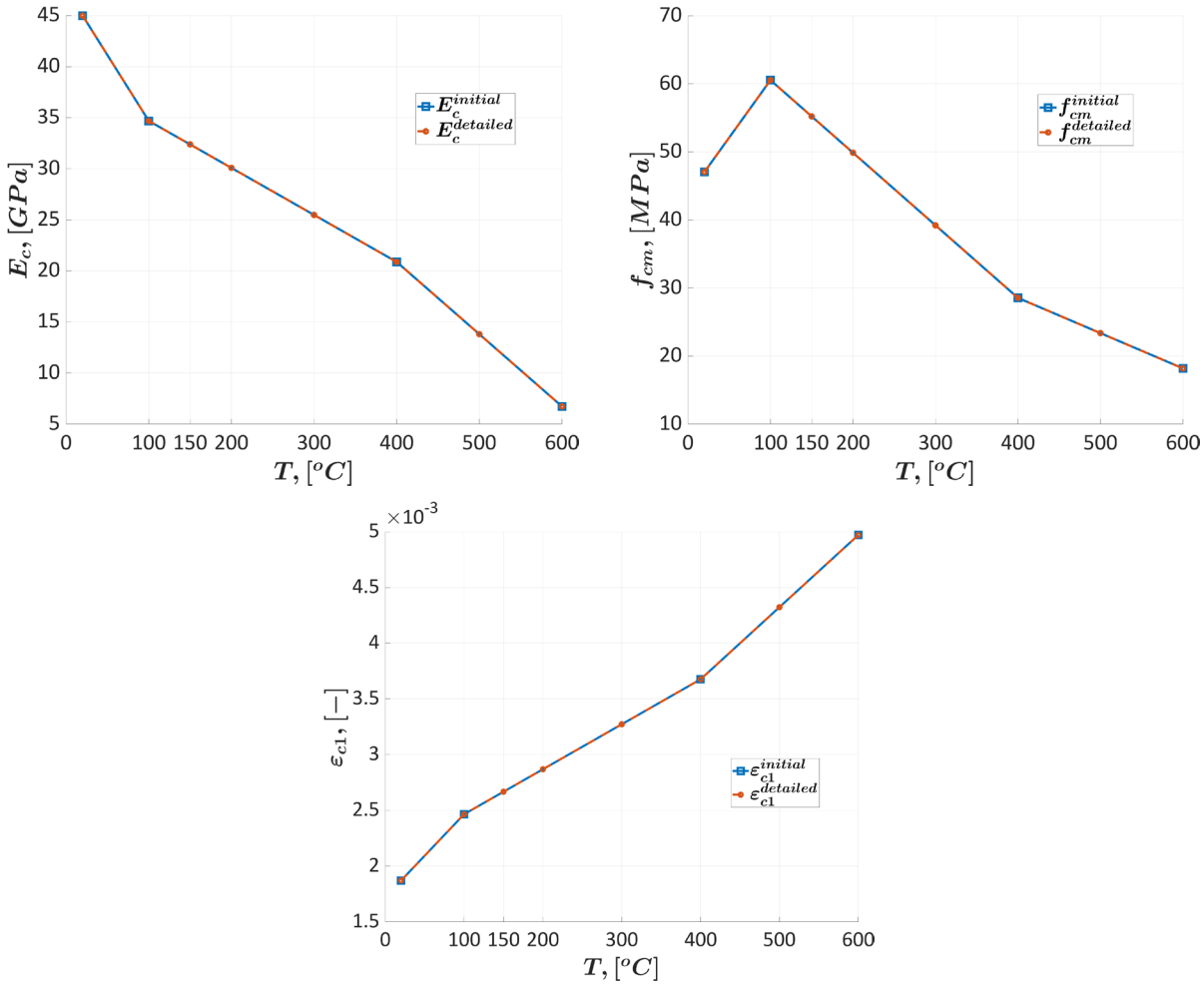

Figure 10. Interpolation of basic physical and mechanical characteristics on an extended temperature grid.

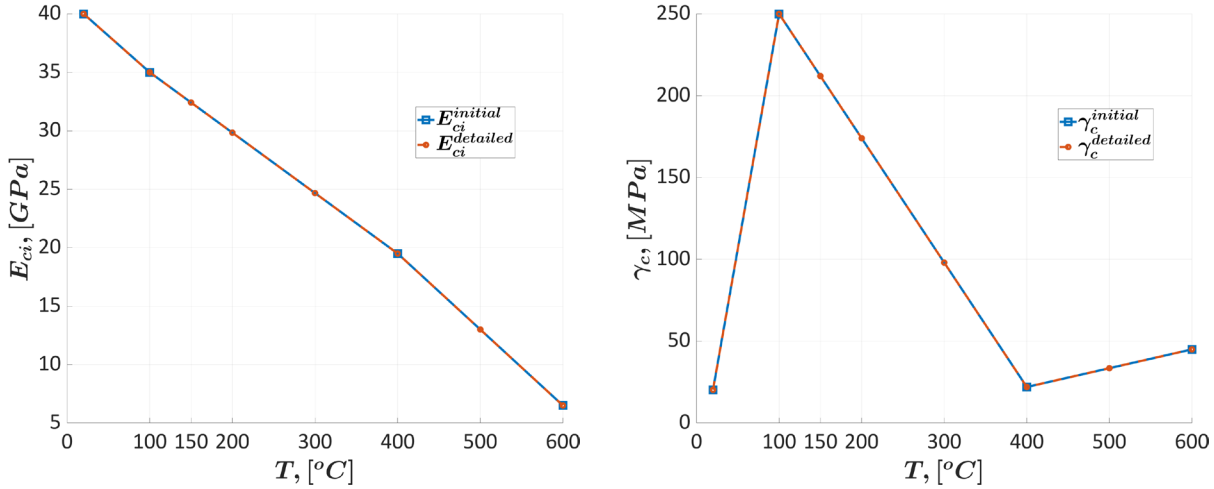

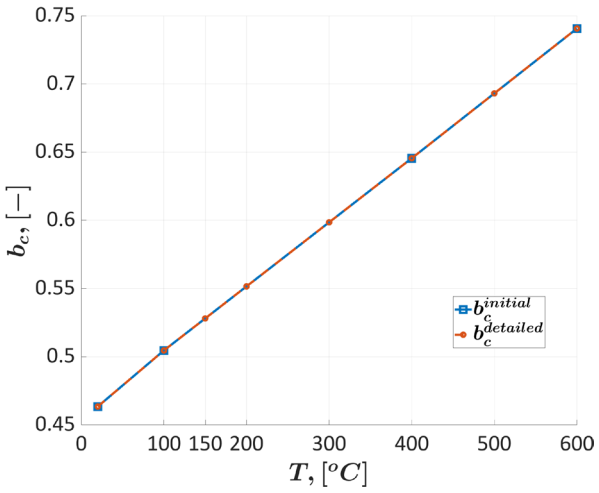

Figure 11. Interpolation of analytical function parameters to an extended temperature grid.

Here, the index "initial" indicates constants that have been identified based on experimental data for temperatures of 20, 100, 400, and 600 °C, and the index "detailed" indicates constants that have been interpolated to an extended value of temperatures of 20, 100, 150, 200, 300, 400, 500, and 600 °C.

In Table 1, the results of identifying for all parameters are shown.

Table 1. Summary table of identification results.

Temperature	20 °C	100 °C	150 °C	200 °C	300 °C	400 °C	500 °C	600 °C
E_c, [GPa]	44.9916	34.6872	32.3861	30.0849	25.4826	20.8802	13.8075	6.73477
f_{cm}, [MPa]	47.0642	60.5492	55.2167	49.8842	39.2192	28.5542	23.3732	18.1922
$\varepsilon_{c1}\cdot 10^3$, [–]	1.87101	2.46612	2.66787	2.86961	3.27309	3.67657	4.32343	4.97028
E_{ci}, [GPa]	40.0000	35.0000	32.4167	29.8333	24.6667	19.5000	13.0000	6.50000
γ_c, [MPa]	20.3100	250.000	212.000	174.000	98.0000	22.0000	33.5000	45.0000
b_c, [–]	0.46357	0.50465	0.52814	0.55163	0.59861	0.64559	0.693165	0.74074
Y_1	0.00792	0.10066	–	–	–	0.10495	–	0.05962
Y_2	0.00735	0.01174	–	–	–	0.01048	–	0.00954
Y_3	5.91e–5	3.27e–5	–	–	–	8.11e–5	–	3.64e–5
Y	0.00866	0.11244	–	–	–	0.11551	–	0.06920

The dependencies shown in Figs. 7 and 9 can be fully used to verify the numerical calculation method in the ABAQUS FEA. Figs. 12 and 13 show the extended compression strain values of the corresponding dependencies family.

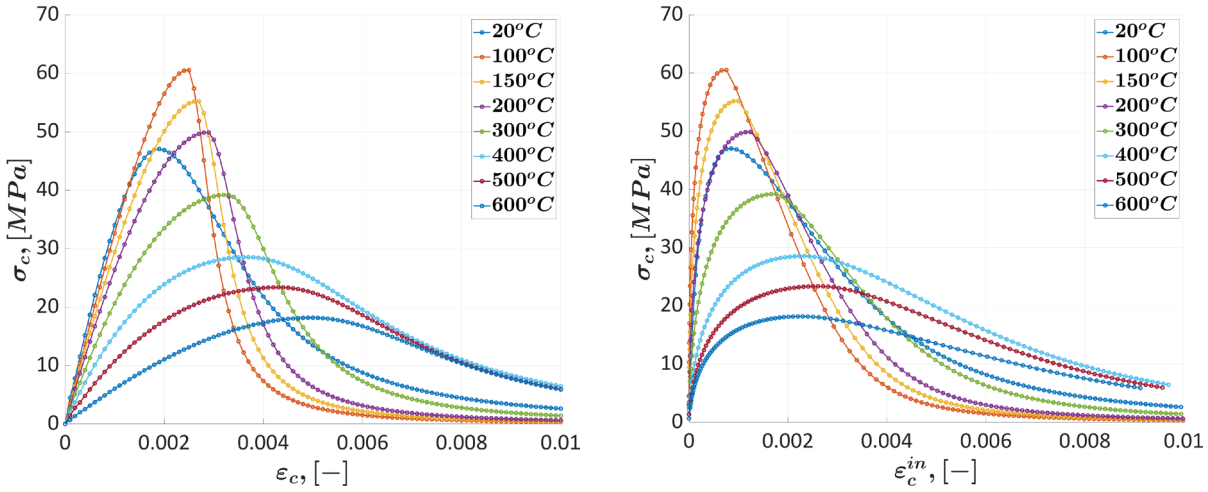

Figure 12. Stress-strain curves family: $\sigma_c(\varepsilon_c, T)$ (left), $\sigma_c(\varepsilon^{in}{}_c, T)$ (right).

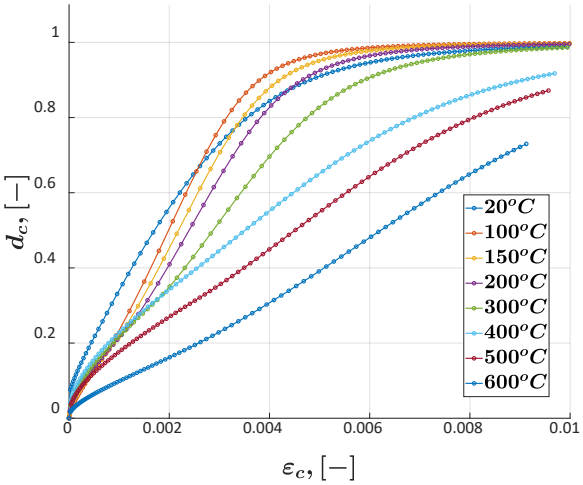

Figure 13. Scalar damage variable family curves $d_c(\varepsilon^{in}{}_c, T)$.

3. Results and Discussion

3.1. Verification of the CDP Model with Identified Parameters

Fig. 14 shows the formulation of the problem in the ABAQUS FEA for a prismatic concrete sample with dimensions of 70×70×280 mm. In addition to the concrete sample, the model contains steel plates with linear-elastic properties. Density of steel is ρ_{steel} = 7850 kg/m^3, Young modulus is E_{steel} = 200 GPa, Poisson's ratio is ν_{steel} = 0.3. To determine the mechanical properties, it is advisable to model a concrete specimen with a single finite element. In this case, the sample is perceived as a sample of the material, and not as a structure.

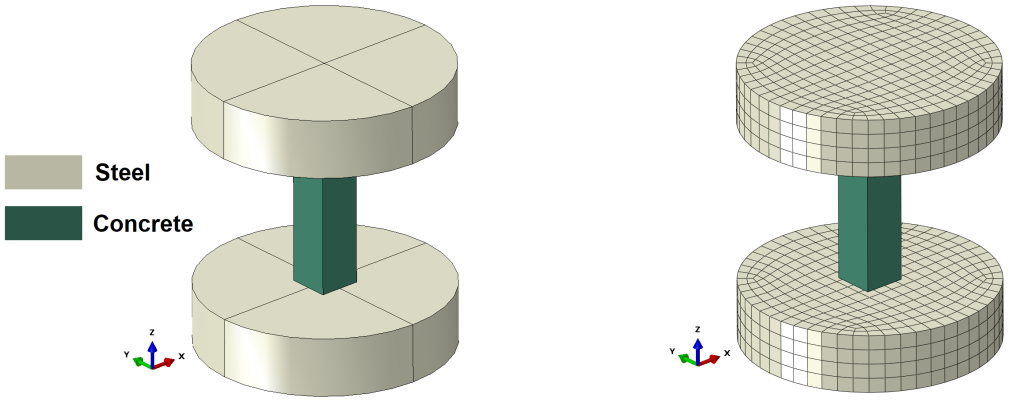

Figure 14. Geometric (left) and finite element (right) model.

In addition to the basic properties, in order to stabilize the applied explicit numerical integration scheme (ABAQUS/EXPLICIT solver), the concrete model also takes into account Rayleigh damping according to the relations (14).

$$\frac{\alpha}{2\omega_i}+\frac{\beta\omega_i}{2}=\xi_i, \tag{14}$$

where α is the coefficient of mass matrix; β is the coefficient of stiffness matrix; ω_i is the i-th natural frequency; ξ_i is the damping coefficient by i-th natural frequency and its value assumed to be equal 0.1.

In this formulation, only damping proportional to the mass is considered, based on the lowest and unique frequency of oscillations of the sample as a rod within the single-element model, so it can be assumed that β = 0. In turn, the first natural frequency of the concrete sample with the given dimensions and properties will be found according to expression (15).

$$\omega_1 = \frac{\pi}{2l}\sqrt{\frac{E_c}{\rho_{concrete}}}. \quad (15)$$

The temperature is set on the concrete element to detect differences in behavior due to properties change. For verification, it is proposed to compare the sample response obtained by calculation with the analytical stress-strain curves specified as material properties for temperature values of 20 and 100 °C.

Fig. 15 shows the boundary conditions in the model. The lower surface of the steel plate is rigidly fixed in space, and the upper surface is connected to the master node, which moves in proportion to the cube of time $u_z \sim t^3$ (kinematic loading) throughout the loading step. Cubic dependence is used for the smooth increase in the acceleration of the plate movement.

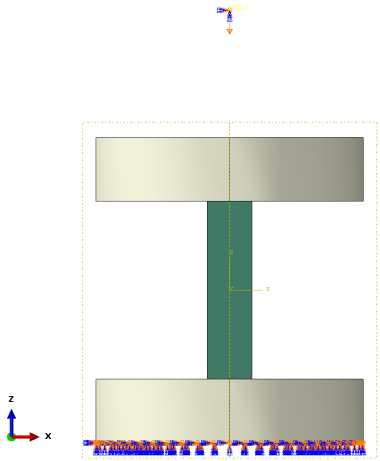

Figure 15. Boundary conditions.

The calculation is carried out in the "*Dynamic Explicit*" formulation. In the case of uniaxial loading, the displacement value (16) corresponding to the final total strain value for the respective temperature shall be applied to the master-node.

$$\varepsilon_c = \frac{u_z}{l}, \quad (16)$$

where u_z is the absolute vertical displacement of the master-node; l is the initial length of specimen.

For cyclic loading, the total calculation time is divided by the number of cycles, and the calculation of each cycle is done independently, but with the initial state of the previous cycle. This can be implemented using "*initial state*" technology in the ABAQUS FEA. Moreover, the resulting displacement value applied to the master-node is also distributed equally across the cycles. However, for this it is necessary not only to divide the total displacement by the number of cycles but also to take into account the accumulated strain.

An important point in the calculation for a sign-constant cyclic load is force control, since it is necessary to stop the calculation at the desired value, without entering the tension region. To do this, it is suggested to modify the ABAQUS keyword file. Moreover, using the "*initial state*" technology, it is possible to set different values of stop force at each load cycle. A description of the commands that should be added to the keyword-file is shown in Table 2.

Table 2. ABAQUS keyword-file modification.

***EXTREME VALUE, HALT=YES**	The "YES" parameter meets the requirement to stop calculation when the critical value is reached.
***EXTREME NODE VALUE, NSET=RP2, MAX**	The calculation stops when the maximum value "MAX" of the monitored value is reached in a set of nodes named "RP2".
RF3, 0.0	The calculation stops when the vertical force reaction "RF3" reaches a value of "0.0" in a set of nodes named "RP2".

At the end of the calculation, information about the reaction, as well as about the displacement, is taken from the master-node, which is converted by scaling into stress and strain according to the ratios (16) and (17).

$$\sigma_c = \frac{R_z}{A}, \tag{17}$$

where R_z is the vertical force reaction in the master-node, A is the cross-sectional area of the specimen.

Then the stress-strain curves are compared – specified as a material properties and obtained from the calculations one.

3.2. Results of Calculations for Uniaxial Compression

Fig. 16 shows a comparison of the uniaxial compression response of a concrete specimen in ABAQUS with the initial, analytically determined, stress-strain curve for temperatures of 20 and 100 °C.

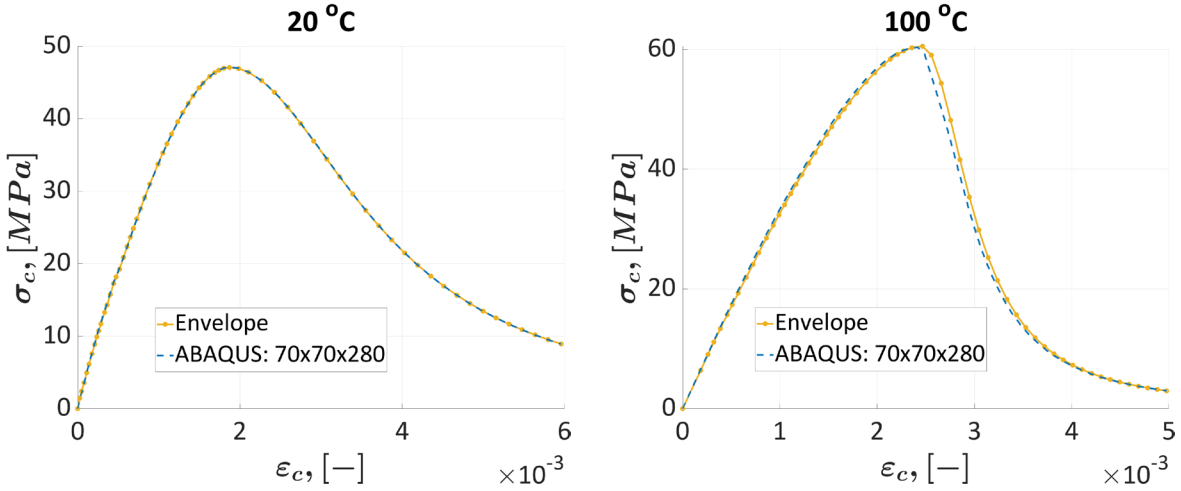

Figure 16. Comparison of calculations: 20 °C (left), 100 °C (right).

There is a complete correspondence of the obtained result with the analytically specified stress-strain curve.

3.3. Results of Calculations for Cyclic Loading

Figs. 17 and 18 show the results of the calculation for cyclic loading. The number of cycles for assessing the degradation of initial elastic properties varied, and options for different values of the reaction in the master-node at which the calculation stops were considered.

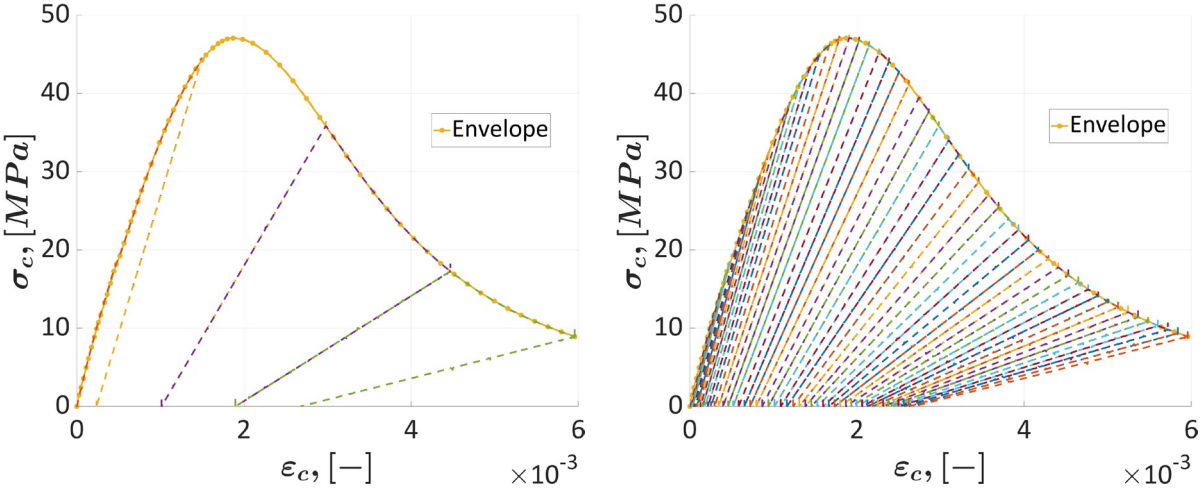

Figure 17. Cyclic load calculation results: 4 cycles with discharge up to 0 kN (left), 50 cycles with unloading up to 0 kN (right)

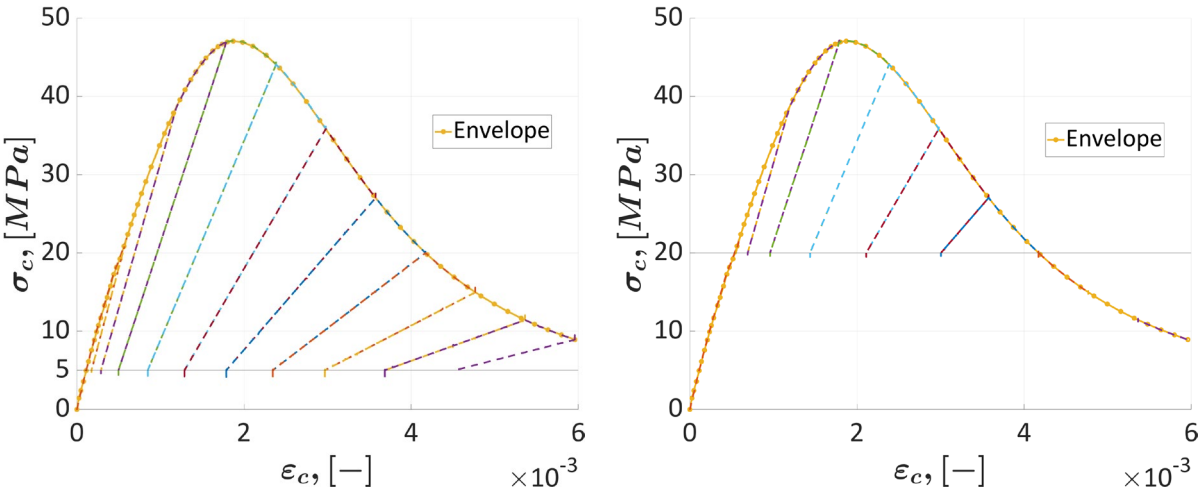

Figure 18. Cyclic load calculation results: 10 cycles with unloading up to 24.5 kN (left), 10 cycles with unloading up to 98 kN (right)

As can be seen from the presented results, under cyclic loading, the general contour of the stress-strain coincides with the initial one, analytically approximated based on experiments [26]. It should be noted that the procedure for stopping the calculation at a given value of vertical force reaction demonstrates its viability. When unloading to force values less than any value on the envelope, the calculation continues two branches of the calculation in the cycle – both for loading and unloading. In turn, when unloading to force values greater than the value on the envelope, the unloading branch is not included, and the calculation follows further along the loading path.

It can also be noted that the results obtained reflect the global practice of modeling inelastic deformation of concrete [4–6, 15–21]. The main aspects of nonlinear behavior under uniaxial and cyclic loading are observed, the temperature dependence of mechanical properties is taken into account, and the behavior of materials with a granular structure in terms of degradation of primary properties (fracture) is taken into account.

4. Conclusions

The paper demonstrates the validation of the CDP mathematical model of nonlinear deformation and strength using the ABAQUS FEA. Using hardware and software complex and test equipment developed separately for this task, the general mechanical properties of heat-resistant concrete were determined, obtained during experiments on cyclic sign-constant loading after exposure to high temperatures. With the help of analytical approximations, the appearance of stress-strain curves, as well as curves of scalar damage (stiffness degradation) variable for different temperatures, was restored.

The proposed methods for identifying parameters make it possible to fully construct a ready-made mathematical model in the MATLAB environment, the input to which is sufficient to provide the initial experimental data. The process of identifying parameters is accompanied by well-known statistical indicators. At the same time, the analytical forms of approximation eliminate the shortcomings associated with the physical nature of the values.

An important aspect of solving the problems of mechanics of a deformable solid is the presence of inhomogeneous, including high-gradient, temperature fields, which significantly affect the physical and mechanical properties of materials and the behavior of structures. Often, when operating under limited data, it is necessary to obtain dependencies for intermediate temperature values. Using the linear interpolation method based on the proposed analytical dependencies, a family of curves for an extended temperature grid was obtained.

In conclusion, the verification problem for uniaxial cyclic sign-constant loading was implemented. The problem was solved for a concrete sample with fixed dimensions. Finite-element formulation implied single-element mesh subdivision. The validity of this solution lies in the fact that in the case of multi-element subdivision, the tested object ceases to be interpreted as a sample, but is a construction of a non-trivial form. This approach also has the right to exist, but often the increase in the number of elements is associated with side effects and, as a result, this can lead to distorted results.

The results obtained on the verification task showed full compliance of the material model with its initial characteristics based on experimental data.

References

1. Rabotnov, Yu.N. O mekhanizme dlitelnogo razrusheniia [On the mechanism of long-term destruction]. Voprosy prochnosti materialov i konstrukciy [Issues of Strength of Materials and Structures]. M.: Ak. Nauk SSSR. 1959. Pp. 5–7.
2. Kachanov, L.M. Osnovy mekhaniki razrusheniia [Foundations of Fracture Mechanics]. M: Nauka. 1974. 312 p.
3. Karpenko, N.I. Obschie modeli mekhaniki zhelezobetona [General models of reinforced concrete mechanics]. M: Stoijizdat. 1996. 416 p.
4. Watanabe, K., Niwa, J., Yokota, H., Iwanami, M. Experimental Study on Stress-Strain Curve of Concrete Considering Localized Failure in Compression. Journal of Advanced Concrete Technology. 2004. 2(3). Pp. 395–407. DOI: 10.3151/jact.2.395
5. Benin, A., Semenov, S., Semenov, A, Bogdanova, G. Parameter identification for coupled elasto-plasto-damage model for overheated concrete. MATEC Web of Conferences. 2017. 107. Article no. 00042. DOI: 10.1051/matecconf/201710700042
6. Benin, A.V., Semenov, A.S., Semenov, S.G., Beliaev, M.O., Modestov, V.S. Methods of identification of concreteelastic-plastic-damage models. Magazine of Civil Engineering. 2017. 8(76). Pp. 279–297. DOI: 10.18720/MCE.76.24
7. Karpenko, N.I., Eryshev, V.A., Latysheva, E.V. Stress-strain Diagrams of Concrete Under Repeated Loads with Compressive Stresses. 2015. 111. Pp. 371–377. DOI: 10.1016/j.proeng.2015.07.103
8. Wang, H., Li, L., Du, X. A thermo-mechanical coupling model for concrete including damage evolution. International Journal of Mechanical Sciences. 2024. 263. Article no. 108761. DOI: 10.1016/j.ijmecsci.2023.108761
9. Lubliner, J., Oliver, J., Oller, S., Onate, E. A plastic-damage model for concrete. International Journal of Solids and Structures. 1989. 25(3). Pp. 299–326. DOI: 10.1016/0020-7683(89)90050-4
10. Lee, J.H., Fenves, G.L. Plastic-Damage Model for Cyclic Loading of Concrete Structures. Journal of Engineering Mechanics. 1998. 124. Pp. 892–900.
11. Lei, B., Qi, T., Li, Y., Jin, Zh., Qian, W. An enhanced damaged plasticity model for concrete under cyclic and monotonic triaxial compression. European Journal of Mechanics – A/Solids. 2023. 100. Article no. 104999. DOI: 10.1016/j.euromechsol.2023.104999
12. Kakavand, M.R.A., Taciroglu, E. An enhanced damage plasticity model for predicting the cyclic behavior of plain concrete under multiaxial loading conditions. Frontiers of Structural and Civil Engineering. 2020. 14(6). Pp. 1531–1544. DOI: 10.1007/s11709-020-0675-7
13. Budarin, A.M., Rempel, G.I., Kamzolkin, A.A., Alekhin, V.N. Concrete damage–plasticity model with double independent hardening. Vestnik MGSU [Monthly Journal on Construction and Architecture]. 2024. 19(4). Pp. 527–543. DOI: 10.22227/1997-0935.2024.4.527-543
14. Abaqus [Online]. URL: https://docs.software.vt.edu/abaqusv2025/English/?show=SIMULIA_Established_FrontmatterMap/sim-r-DSDocAbaqus.htm (reference date:19.10.2025).
15. Fakeh, M., Jawdhari A., Fam A. Recommended concrete damage plasticity parameters and constitutive models for UHPC in ABAQUS. Engineering Structures. 2025. 333. Article no. 120154. DOI: 10.1016/j.engstruct.2025.120154
16. Rainone, L.S., Tateo, V., Casolo, S., Uva, G. About the Use of Concrete Damage Plasticity for Modeling Masonry Post-Elastic Behavior. Buildings. 2023. 13. Article no. 1915. DOI: 10.3390/buildings13081915
17. Bayat, H., Chalecki, M., Lesniewska, A., Maj, M., Rybak, J., Ubysz, A. The cyclic load effect on the elasticity and plasticity deformation of high-strength reinforced concrete elements. Archives of Civil and Mechanical Engineering. 2024. 24. Article no. 135. DOI: 10.1007/s43452-023-00855-9
18. Lovlev, G., Zileev, A.G. Concrete Damage Plasticity model testing in numerical modeling of cemented rock fill. Gornyi Zhurnal. 2025. 9. Pp. 77–97. DOI: DOI: 10.17580/gzh.2025.09.10
19. Dewi, P.A.P, Sudarsana, I.K., Susila, I.G.A. Validation control in finite element analysis of wide beam-column connections using concrete damage plasticity under cyclic loading. Journal of Infrastructure Planning and Engineering. 2025. 4(1). Pp. 1–3. DOI: 10.22225/jipe.4.1.2025.1-9
20. Hu, A., Chen, X., Du, X., Wang, F. Dynamic Compressive Damage Constitutive Correction of Concrete Under Freeze-Thaw Cycle. Materials. 2025. 18(6). Article no. 1238. DOI: 10.3390/ma18061238
21. Feng, W., Hussin, T.A.R., Yang, X. A temperature-indexed concrete damage plasticity framework for thermomechanical analysis of concrete structures. Journal of Engineering and Applied Science. 2025. 72. Article no. 177. DOI: 10.1186/s44147-025-00753-2
22. Jankowiak, T., Lodygowski, T. Identification of parameters of concrete damage plasticity constitutive model. Foundations of civil and environmental engineering. 2005. 6. Pp. 53–69.
23. Hafezolghorani, M., Hejazi, F., Vaghei, R., Jaafar, M.S.B., Karimzade, R. Simplified Damage Plasticity Model for Concrete. Structural Engineering International. 2017. 27(1). Pp. 68–78. DOI: 10.2749/101686616X1081
24. Rakić, D.M., Bodić, A.S., Milivojević, N.J., Dunić, V.L., Živković, M.M. Concrete damage plasticity material model parameters identification. Journal of the Serbian Society for Computational Mechanics. 2021. 15(2). Pp. 111–122. DOI: 10.24874/jsscm.2021.15.02.11
25. Alfarah, B., López-Almansa, F., Oller, S. New methodology for calculating damage variables evolution in Plastic Damage Model for RC structures. Engineering Structures. 2017. 132. Pp. 70–86. DOI: 10.1016/j.engstruct.2016.11.022
26. Birtel, V., Mark, P. Parameterised Finite Element Modelling of RC Beam Shear Failure. Proceedings of the ABAQUS Users' Conference. 2006. 14. Pp. 95–108.
27. Niu, Y., Wang, W., Su, Y., Jia, F., Long, X. Plastic damage prediction of concrete under compression based on deep learning. Acta Mechanica. 2024. 235. Pp. 255–266. DOI: 10.1007/s00707-023-03743-8
28. Murtazin, I.R., Melnikov, B.E., Semenov, A.S. Simulation of Inelastic Response of Polycrystalline Nickel Based on Micromechanical Model Homogenization. Advanced Problem in Mechanics III. Springer. Cham, 2023. Pp. 427–444. DOI: 10.1007/978-3-031-37246-9_32
29. Yurchenko, V.V., Peleshko, I.D. Improved gradient projection method for parametric optimisation of bar structures. Magazine of Civil Engineering. 2020. 6(98). Article no. 9812. DOI: 10.18720/MCE.98.12
30. Tiraturyan, A.N., Uglova, E.V., Simchuk, E.N., Kadyrov, G.F., Gorskiy, M.Yu. Prediction of temperature distribution in asphalt concrete layers. Magazine of Civil Engineering. 2024. 17(7). Article no. 13101. DOI: 10.34910/MCE.131.1

31. Lukash, K.A., Shurshilin, E.A., Olekhnovich, Y.A., Radaev, A.E. Correlation model for cost and technical characteristics of thermal insulation material used in enclosing structure. Magazine of Civil Engineering. 2025. 18(1). Article no. 13306. DOI: 10.34910/MCE.133.6

Information about the authors:

Ilnar Murtazin,
ORCID: https://orcid.org/0000-0002-7580-5669
E-mail: murtazin_ir@spbstu.ru

Roman Fedorenko,
ORCID: https://orcid.org/0000-0002-2115-1751
E-mail: fedorenko_rv@spbstu.ru

Aleksei Lukin, *PhD in Physics and Mathematics*
ORCID: https://orcid.org/0000-0003-2016-8612
E-mail: lukin_av@spbstu.ru

Victor Modestov, *PhD in Technical Sciences*
ORCID: https://orcid.org/0000-0003-0845-638X
E-mail: vmodestov@spbstu.ru

Andrey Malinkin, *PhD in Technical Sciences*
E-mail: mas193cm@mail.ru

Mikhail Fedotov,
E-mail: domzagorodom@mail.ru

Sergey Panarin, *PhD in Technical Sciences*
E-mail: tekhnoarm@mail.ru

Received 19.06.2025. Approved after reviewing 12.09.2025. Accepted 12.09.2025.